Journal of Naval Architecture and Marine Engineering
July, 2025
http://dx.doi.org/10.3329/jname.v22i2.75405 *http://www.banglajol.info*

NONLINEAR UNSTEADY MHD FLOW IN AN INCLINED CHANNEL WITH SUCTION AND HEAT GENERATION: TIME PERIODIC BOUNDARY CONDITIONS

M. Venkateswarlu[1*], P. Rami Reddy[2] and K. Jaya Lakshmi[3]
[1]Department of Mathematics, Siddhartha Academy of Higher Education, Vijayawada, Andhra Pradesh, India, PIN : 520 007.
[2]Department of Mathematics, Krishna University, Machilipatnam, Andhra Pradesh, India, PIN : 522 237.
[3]Department of Mathematics, JNTUA University, Anantapur, Andhra Pradesh, India, PIN : 515 002.
*Email : mvsr2010@gmail.com

Abstract:
This paper is presented to analyze the task of assimilating parameters on MHD flow structure in a sloped pipeline while certain plate is disorderly heated. The impact of suction and heat generation is considered. The dictating liquid motion and energy equations are ascertained and corresponding expressions for thermal energy, liquid motion, fanning friction and stress flatten are acquired. In particular, the liquid motion behaves an increasing function of suction parameter and a decreasing function of magnetic parameter. This research is of special consequence in marine steam engineering, naval ships mooring and replenishment, medicine, and aerodynamics. Results are verified in special case with those existing in the literature.

Keywords: Mixed convection, hydromagnetic, suction, heat generation, time periodic boundary conditions

NOMENCLATURE

A	function of y and t
B	function of t
B_0	uniform magnetic field
C	nonlinear Bousssinesq approximation parameter
c_p	specific heat at constant pressure
D	hydraulic diameter (m)
f_1	fanning friction factor at the plate $y=-h$
f_2	fanning friction factor at the plate $y=h$
g	gravitational acceleration $\left(m s^{-2}\right)$
Gr	Grashof number
H	heat generation parameter
h	half of the channel width (m)
k	thermal conductivity $\left(W m^{-1} K^{-1}\right)$
M	magnetic parameter
Nu	Nusselt number
p	difference between the pressure and the hydrostatic pressure
P	pressure (Pa)
Pr	Prandtl number
Q_0	dimensional heat generation parameter
q	heat flux per unit area
Re	Reynolds number
S	suction parameter
t	dimensional time (s)
T	temperature (K)
T_0	mean temperature in a channel section (K)
T_1	temperature of the plate at $y=-h$ (K)
T_2	temperature of the plate at $y=h$ (K)
U	non-dimensional velocity $\left(m s^{-1}\right)$
u	dimensional velocity $\left(m s^{-1}\right)$
u_0	mean velocity in a channel section $\left(m s^{-1}\right)$
V_0	scale of suction velocity $\left(m s^{-1}\right)$
x,y	rectangular coordinates (m)

Greek Symbols

α	thermal diffusivity
β	volumetric coefficient of thermal expansion
η	non-dimensional coordinate (m)
τ	non-dimensional time (s)
θ	non-dimensional temperature (K)
λ	non-dimensional pressure drop
ν	kinematic viscosity
ρ	mass density $\left(Kg m^{-1}\right)$
σ	liquid electrical conductivity (S/m)

1813-8535 (Print), 2070-8998 (Online) Received on: August, 2024

ρ_0	mass density for $T = T_0$ $\left(Kg\,m^{-1}\right)$	ω	dimensional angular frequency (Hz)
ϕ	tilt angle (rad)	Ω	non-dimensional angular frequency (Hz)

1. Introduction

Scientists are interrogating the application of MHD in distinct fields, such as cancer treatments, executing digestive system concern, therapeutic control of magnets, MRI scans, cavity sorting instruments, targeted drug transmission with magnets, and in moving disordered biological waste liquids. MHD has industrial applications including in MHD generators, creating particular metal alloys, MHD sensors, solar power collection, and nuclear waste processing. Makinde and Onyejekwe (2011) discussed the MHD generalized Couette flow and heat transfer with variable viscosity and electrical conductivity. Narasimhan (2011) presented the flow of an electrically conducting nonlocal viscous fluid between parallel plates in the proximity of a transverse magnetic field in MHD. Venkateswarlu et al. (2020) reported the thermodynamics analysis of Hall current and Soret number on hydromagnetic couette flow in a rotating system with a convective boundary condition. Jha et al (2022) studied the Run up flow of MHD fluid between parallel Porous plates in the presence of transverse magnetic field. Indira and Raju (2023) presented the MHD mixed convection flow for Maxwell Nanofluid through a vertical cone with porous material in the presence of variable thermal conductivity. Raghunath et al. (2023) discussed the radiation absorption on MHD free conduction flow through porous medium over an unbounded vertical plate with heat source. Prasad et al. (2023) examined the unsteady MHD free convective fluid flow past an inclined porous plate with chemical reaction, viscous dissipation and radiation absorption effects. Venkateswarlu et al. (2022) reported the impulsive and accelerated motions of Casson fluid in an inclined plate in the proximity of MHD and heat generation. Nagesh and Raghunath (2022) discussed the Soret, radiation and chemical reaction effect on MHD Jeffrey fluid flow past an inclined vertical plate embedded in porous medium. Kumar et al. (2024) presented the MHD and heat transfer characteristics of thermally radiative upper convective Maxwell fluid flow between moving plates. Rajakumar et al. (2024) discussed the impact of concentration gradient-induced heat flow on unsteady MHD heat and mass transform dissipative flow with slantwise temperature fluctuations.

Suction or blowing plays a significant task for examining the dispersal mechanism of solute through distinct flow field. Suction or injection has been extensively designed in boundary layers, but less so in channel flows. Obalalu et al. (2020) reported the heat transfer in an unsteady vertical porous channel with injection/suction in the presence of heat generation. Fardi et al. (2021) presented the MHD suction–injection model of viscous fluid using a kernel-based method. Venkateswarlu and Lakshmi (2021) examined the diffusion-thermo and heat source effects on the unsteady radiative MHD boundary layer slip flow past an infinite vertical porous plate. Marzieh et al. (2021) studied the combined effect of roughness and suction on heat transfer in a laminar channel flow. Raghunatha and Vinod (2023) presented the effects of heat transfer on MHD suction or injection model of viscous fluid flow through differential transformation and Bernoulli wavelet techniques. Susmita et al. (2024) analyzed the effects of suction/injection and Reynolds number on the transport process in a hydromagnetic flow through a channel of reactive porous walls. Adem and Chanie (2024) discussed the influence of suction and injection on the electrical MHD behavior of nanofluid in a nonlinear radiative flow over an extending surface. Sivaprasad and Kumar (2025) discussed the MHD of laminar viscous fluid flow over a contaminated liquid drop in a porous area.

The mixed convection stream problem between two proportionate plates has established immeasurable recognition during the last several years. The research has indicative applications in the domain of radial diffusers, computer container devices, lubrication, and petroleum industries etc. Avci and Aydin (2007) presented the mixed convection in a vertical parallel plate microchannel with asymmetric wall heat fluxes. Jha et al. (2015) discussed the mixed convection in an inclined channel filled with porous material having time-periodic boundary conditions. Venkateswarlu and kumar (2017) reported the Soret and heat source effects on MHD flow of a viscous fluid in a parallel porous plate channel in presence of slip condition. Venkateswarlu and Lakshmi (2017) studied the thermal diffusion, hall current and chemical reaction effects on unsteady MHD natural convective flow past a vertical plate. Makinde et al. (2018) discussed the unsteady MHD flow of radiating and rotating fluid with Hall current and thermal diffusion past a moving plate in a porous medium. Venkateswarlu and Makinde (2018) presented the unsteady MHD slip flow with radiative heat and mass transfer over an inclined plate embedded in a porous medium. Hamza et al. (2019) reported the mixed convection flow of viscous reactive fluids with thermal diffusion and radial magnetic field in a vertical porous annulus. Meduri and Devi (2024) reported the stokes flow past a contaminated fluid sphere embedded in a porous medium with slip condition. Venkateswarlu et al. (2024) discussed the Soret and Dufour effects on heat destructive Casson

liquid movement past an infinite vertical plate. Reddy and Sreedevi (2024) discussed the magnetic nano-encapsulated phase change materials for latent heat thermal energy storage: Enhanced entropy generation and heat transfer characteristics.

The aspiration of this article is to present an extensive conceptual study of a nonlinear mixed convection unsteady MHD motion with suction in a slanted channel constructed by two indefinite proportionate plates. Numerous considerable employments are associated to the current contribution especially as polymer extrusion, liquid motion in Earth's facade, cooling of molten liquid, star conformation, construction of a glass plate.

2. Mathematical Model

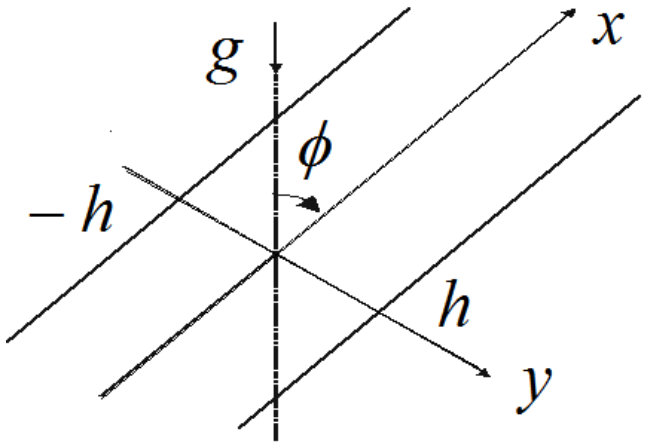

Fig. 1: Sketch of the inclined channel.

Let us imagine the laminar, two dimensional motion of an incompressible and viscous liquid between two indefinite proportionate plates. The $x-$axis is taken vertically upward direction and the $y-$axis is taken normal to the plates as shown in Figure 1. The liquid is controlled by two proportionate plates compartmentalized by a distance $2h$, which are inclined with reference to the gravitational acceleration g. A uniform magnetic field of strength B_0 is applied normal to the plates. The plates are supposed to be stagnant and the temperature at the plate $y=-h$ is preserved isothermally with temperature T_1 whereas the plate at $y=h$ is reference to periodic temperature as [See, Barletta and Zanchini (2003)]:

$$T(x,h,t)=T_2+(T_2-T_0)\cos(\omega t) \tag{1}$$

In addition to, the motion is supposed to be thermally and hydrodynamically fully refined, so that heat flow takes place in the transverse direction only, such that $\partial T/\partial x=\partial u/\partial x=0$. The nonlinear Boussinesq simulation [See, Barletta and Zanchini (2003); Jha and Oni (2020)] is generated; which is substantial while the temperature variation between the channel plates is noticeably large. The nonlinear equation of state is obtained by expanding the Boussinesq simulation up to second degree polynomial as:

$$\rho=\rho_0\left[1-\beta_0(T-T_0)-\beta_1(T-T_0)^2\right] \tag{2}$$

where T_0 is a mean temperature with reference to both the period $0\le t\le 2\pi/\omega$ and the interval $-h\le y\le h$

$$T_0=\frac{\omega}{4\pi h}\int_0^{2\pi/\omega}\int_{-h}^{h} T\,dy\,dt \tag{3}$$

Moreover, to a steady mass flow rate is predetermined; hence an average motion in a channel section, can be expressed as

$$u_0=\frac{1}{2h}\int_{-h}^{h} u\,dy \tag{4}$$

Omitting the viscous dissipation term in the energy equation and contributing the nonlinear Boussinesq simulation, in dimensional form, the momentum and energy equations can be expressed as:

$$\frac{\partial u}{\partial t}-V_0\frac{\partial u}{\partial y}=g\left[\beta_0\left(T-T_0\right)+\beta_1\left(T-T_0\right)^2\right]\cos\phi-\frac{1}{\rho_0}\frac{\partial p}{\partial x}+\nu\frac{\partial^2 u}{\partial y^2}-\frac{\sigma B_0^2}{\rho_0}u \tag{5}$$

$$g\beta_0\left(T-T_0\right)\sin\phi+\frac{1}{\rho_0}\frac{\partial p}{\partial y}=0 \tag{6}$$

$$\frac{\partial T}{\partial t}-V_0\frac{\partial T}{\partial y}=\alpha\frac{\partial^2 T}{\partial y^2}+\frac{Q_0}{\rho_0 c_p}\left(T-T_0\right) \tag{7}$$

where $p=P+\rho_0 g\left[x\cos\phi-y\sin\phi\right]$

The no slip boundary restrictions for momentum equation and time periodic boundary restrictions for energy equation, in dimensional form are as follows:

$$u\left(y,t\right)=0,\ T\left(y,t\right)=T_1 \qquad \text{at} \quad y=-h \tag{8}$$

$$u\left(y,t\right)=0,\ T\left(y,t\right)=T_2+\left(T_2-T_0\right)\exp\left(i\omega t\right) \qquad \text{at} \quad y=h \tag{9}$$

Differentiating Eq. (5) with respect to x, we obtain

$$\frac{\partial^2 p}{\partial x^2}=0 \tag{10}$$

Differentiating Eq. (6) with respect to x, we obtain

$$\frac{\partial^2 p}{\partial x\partial y}=0 \tag{11}$$

Using the Eqs. (10) and (11), we obtain

$$p\left(x,y,t\right)=A\left(y,t\right)-xB\left(t\right) \tag{12}$$

Introduce the non-dimensional quantities listed below.

$$U=\frac{u}{u_0},\tau=\omega t,\ D=4h,\ \eta=\frac{y}{D},\ \theta=\frac{T-T_0}{T_2-T_0},\ \chi=\frac{T_2-T_1}{T_2-T_0},\ \xi=\frac{T_1-T_0}{T_2-T_0} \tag{13}$$

Using the Eqs. (12) and (13), Eqs. (5) and (7) can expressed in non-dimensional form as

$$\frac{\partial U}{\partial\tau}-\frac{S}{\Omega}\frac{\partial U}{\partial\eta}=\frac{\lambda}{\Omega}+\frac{1}{\Omega}\frac{Gr}{\mathrm{Re}}\left[\theta+C\theta^2\right]+\frac{1}{\Omega}\frac{\partial^2 U}{\partial\eta^2}-\frac{M^2}{\Omega}U \tag{14}$$

$$\frac{\partial\theta}{\partial\tau}-\frac{S}{\Omega}\frac{\partial\theta}{\partial\eta}=\frac{1}{\Omega\,\mathrm{Pr}}\frac{\partial^2\theta}{\partial\eta^2}+\frac{H}{\Omega}\theta \tag{15}$$

Here $\Omega=\frac{\omega D^2}{\nu}$ is the frequency of the oscillating temperature, $S=\frac{V_0 D}{\nu}$ is the suction parameter, $M^2=\frac{\sigma B_0^2 D^2}{\rho_0\nu}$ is the Hartmann parameter, $\lambda=\frac{D^2 B}{\mu u_0}$ is the pressure gradient in the liquid, $Gr=\frac{g\,\beta_0\left(T_2-T_0\right)D^3\cos\phi}{\nu^2}$ is the Grashof number, $Re=\frac{u_0 D}{\nu}$ is the Reynolds number, $C=\frac{\beta_1\left(T_2-T_0\right)}{\beta_0}$ is the nonlinear Boussinesq simulation parameter, $H=\frac{Q_0 D^2}{\nu\rho_0 c_p}$ is the heat generation parameter, and $Pr=\frac{\nu}{\alpha}$ is the Prandtl number respectively.

The boundary restrictions in non-dimensional pattern can be expressed as

$$U\left(\eta,\tau\right)=0,\ \theta\left(\eta,\tau\right)=\xi \qquad \text{at} \quad \eta=-\frac{1}{4} \tag{16}$$

$$U\left(\eta,\tau\right)=0,\ \theta\left(\eta,\tau\right)=\xi+\chi+\exp\left(i\tau\right) \qquad \text{at} \quad \eta=\frac{1}{4} \tag{17}$$

The following constraints on the functions $U\left(\eta,\tau\right)$ and $\theta\left(\eta,\tau\right)$, can be obtained by Eqs. (3-4)

$$\int_{-1/4}^{1/4} U(\eta,\tau)\,d\eta = \frac{1}{2} \tag{18}$$

$$\int_{0}^{2\pi}\int_{-1/4}^{1/4} \theta(\eta,\tau)\,d\eta\,d\tau = 0 \tag{19}$$

Differentiating equation (18) with respect to τ on both sides, we get

$$\int_{-1/4}^{1/4} \frac{\partial}{\partial\tau} U(\eta,\tau)\,d\eta = 0 \tag{20}$$

Solving Eq. (14) and using Eq. (20), we can obtain

$$\frac{\lambda + S - M^2}{2} + \frac{Gr}{Re}\int_{-1/4}^{1/4}\left(\theta + C\theta^2\right)d\eta = \left[\frac{\partial U}{\partial\eta}\right]_{\eta=-\frac{1}{4}} - \left[\frac{\partial U}{\partial\eta}\right]_{\eta=\frac{1}{4}} \tag{21}$$

The fanning frictional factors at the channel plates $y = -h$ and $y = h$ are defined as

$$f_1 = \frac{2\nu}{u_0^2}\left[\frac{\partial u}{\partial y}\right]_{y=-h} = \frac{2}{Re}\left[\frac{\partial U}{\partial\eta}\right]_{y=-\frac{1}{4}} \tag{22}$$

$$f_2 = -\frac{2\nu}{u_0^2}\left[\frac{\partial u}{\partial y}\right]_{y=h} = -\frac{2}{Re}\left[\frac{\partial U}{\partial\eta}\right]_{y=\frac{1}{4}} \tag{23}$$

Using Eqs. (21-23), one can obtain the connection between the pressure drop and Fanning friction factors as:

$$\lambda + S - M^2 + 2\frac{Gr}{Re}\int_{-1/4}^{1/4}\left(\theta + C\theta^2\right)d\eta = \left(f_1 + f_2\right)Re \tag{24}$$

Using the temperature field, the heat flux per unit area can be expressed as

$$q_w = k_T\frac{\partial T}{\partial y} \tag{25}$$

In non-dimensional pattern, the heat transfer coefficient Nu can be expressed as

$$Nu = \frac{D\,q_w}{k_T\left(T_2 - T_0\right)} \tag{26}$$

Applying non-dimensional quantities in Eq. (13) and Eqs. (25-26), we can obtain

$$Nu = \frac{\partial\theta}{\partial\eta} \tag{27}$$

3. Analytical Solution

Define the complex valued functions $U^*(\eta,\tau)$, $\theta^*(\eta,\tau)$, and $\lambda^*(\tau)$ which can satisfy the following equations

$$\frac{\partial U^*}{\partial\tau} - \frac{S}{\Omega}\frac{\partial U^*}{\partial\eta} = \frac{\lambda^*}{\Omega} + \frac{1}{\Omega}\frac{Gr}{\mathrm{Re}}\left[\theta^* + C\theta^{*2}\right] + \frac{1}{\Omega}\frac{\partial^2 U^*}{\partial\eta^2} - \frac{M^2}{\Omega}U^* \tag{28}$$

$$\frac{\partial\theta^*}{\partial\tau} - \frac{S}{\Omega}\frac{\partial\theta^*}{\partial\eta} = \frac{1}{\Omega\,\mathrm{Pr}}\frac{\partial^2\theta^*}{\partial\eta^2} + \frac{H}{\Omega}\theta^* \tag{29}$$

$$U^*(\eta,\tau) = 0,\ \theta^*(\eta,\tau) = \xi \qquad \text{at} \quad \eta = -\frac{1}{4} \tag{30}$$

$$U^*(\eta,\tau) = 0,\ \theta^*(\eta,\tau) = \xi + \chi + \exp(i\tau) \qquad \text{at} \quad \eta = \frac{1}{4} \tag{31}$$

$$\int_{-1/4}^{1/4} U^*(\eta,\tau)\,d\eta = \frac{1}{2} \tag{32}$$

$$\int_{0}^{2\pi}\int_{-1/4}^{1/4} \theta^*(\eta,\tau)\,d\eta\,d\tau = 0 \tag{33}$$

Here U = Real part of $\left(U^*\right)$, λ = Real part of $\left(\lambda^*\right)$, and θ = Real part of $\left(\theta^*\right)$.

The solutions of Eqs. (28-29) can be expressed in the form

$$U^*(\eta,\tau) = U_a^*(\eta) + \frac{Gr}{Re}U_b^*(\eta)\exp(i\tau) \tag{34}$$

$$\lambda^*(\tau) = \lambda_a^* + \frac{Gr}{Re}\lambda_b^*\exp(i\tau) \tag{35}$$

$$\theta^*(\eta,\tau) = \theta_a^*(\eta) + \theta_b^*(\eta)\exp(i\tau) \tag{36}$$

On substituting Eqs. (34-36) into Eqs. (28-33), we can obtain

$$\frac{d^2U_a^*}{d\eta^2} + S\frac{dU_a^*}{d\eta} - M^2U_a^* + \lambda_a^* + \frac{Gr}{Re}\left[\theta_a^* + C\theta_a^{*2}\right] = 0 \tag{37}$$

$$\frac{d^2U_b^*}{d\eta^2} + S\frac{dU_b^*}{d\eta} - M^2U_b^* + \lambda_b^* + 2C\theta_a^*\theta_b^* + \theta_b^* - i\Omega U_b^* = 0 \tag{38}$$

$$\frac{d^2\theta_a^*}{d\eta^2} + S\,Pr\frac{d\theta_a^*}{d\eta} + H\,Pr\,\theta_a^* = 0 \tag{39}$$

$$\frac{d^2\theta_b^*}{d\eta^2} + S\,Pr\frac{d\theta_b^*}{d\eta} + (H - i\Omega)\,Pr\,\theta_b^* = 0 \tag{40}$$

$$U_a^*(\eta) = 0, U_b^*(\eta) = 0, \theta_a^*(\eta) = \xi, \theta_b^*(\eta) = 0 \qquad \text{at} \quad \eta = -\frac{1}{4} \tag{41}$$

$$U_a^*(\eta) = 0, U_b^*(\eta) = 0, \theta_a^*(\eta) = \xi + \chi, \theta_b^*(\eta) = 1 \qquad \text{at} \quad \eta = \frac{1}{4} \tag{42}$$

$$\int_{-1/4}^{1/4} U_a^*(\eta)\,d\eta = \frac{1}{2}, \quad \int_{-1/4}^{1/4} U_b^*(\eta)\,d\eta = 0 \tag{43}$$

$$\int_{-1/4}^{1/4} \theta_a^*(\eta)\,d\eta = 0 \tag{44}$$

Using the liquid motion, the fanning frictional factor can be expressed as

$$f_{1a}^*\,Re = 2\left[\frac{dU_a^*}{d\eta}\right]_{\eta=-\frac{1}{4}} \tag{45}$$

$$f_{2a}^*\,Re = -2\left[\frac{dU_a^*}{d\eta}\right]_{\eta=\frac{1}{4}} \tag{46}$$

$$f_{1b}^*\,Re = 2\left[\frac{dU_b^*}{d\eta}\right]_{\eta=-\frac{1}{4}} \tag{47}$$

$$f_{2b}^*\,Re = -2\left[\frac{dU_b^*}{d\eta}\right]_{\eta=\frac{1}{4}} \tag{48}$$

Using the temperature domain, the heat transfer coefficient can be expressed as

$$Nu_{1a}^{*}=\left[\frac{d\theta_a^{*}}{d\eta}\right]_{\eta=-\frac{1}{4}} \tag{49}$$

$$Nu_{2a}^{*}=\left[\frac{d\theta_a^{*}}{d\eta}\right]_{\eta=\frac{1}{4}} \tag{50}$$

$$Nu_{1b}^{*}=\left[\frac{d\theta_b^{*}}{d\eta}\right]_{\eta=-\frac{1}{4}} \tag{51}$$

$$Nu_{2b}^{*}=\left[\frac{d\theta_b^{*}}{d\eta}\right]_{\eta=\frac{1}{4}} \tag{52}$$

By integrating Eqs. (37-40) with boundary restrictions (41-44), we can acquired

$$\theta_a^{*}=a_6\,exp\left(-m_1\eta\right)+a_7\,exp\left(-m_2\eta\right) \tag{53}$$

$$\begin{aligned}U_a^{*}=&\frac{\lambda_a^{*}}{M^2}\left[1+a_{15}\,exp\left(-m_5\eta\right)-a_{23}\,exp\left(-m_6\eta\right)\right]+\\&\frac{Gr}{Re}\left[a_{21}\,exp\left(-m_5\eta\right)-a_{29}\,exp\left(-m_6\eta\right)-a_{10}\,exp\left(-m_1\eta\right)-a_{11}\,exp\left(-m_2\eta\right)\right]-\\&a_{12}\,exp\left(-2m_1\eta\right)-a_{13}\,exp\left(-\left(m_1+m_2\right)\eta\right)-a_{14}\,exp\left(-2m_2\eta\right)+\\&a_{22}\,exp\left(-m_5\eta\right)-a_{30}\,exp\left(-m_6\eta\right)\end{aligned} \tag{54}$$

$$\lambda_a^{*}=M^2\left[a_{44}-\frac{Gr}{Re}a_{45}\right] \tag{55}$$

$$\theta_b^{*}=a_8\exp\left(-m_4\eta\right)-a_9\exp\left(-m_3\eta\right) \tag{56}$$

$$\begin{aligned}U_b^{*}=&\frac{\lambda_b^{*}}{M^2+i\Omega}\left[1+a_{52}\,exp\left(-m_7\eta\right)-a_{62}\,exp\left(-m_8\eta\right)\right]+\\&a_{47}\,exp\left(-m_3\eta\right)-a_{46}\,exp\left(-m_4\eta\right)+a_{59}\,exp\left(-m_7\eta\right)+\\&a_{67}\,exp\left(-m_8\eta\right)-a_{48}\,exp\left(-\left(m_1+m_2\right)\eta\right)+a_{49}\,exp\left(-\left(m_1+m_3\right)\eta\right)+\\&a_{51}\,exp\left(-\left(m_2+m_3\right)\eta\right)-a_{50}\,exp\left(-\left(m_2+m_4\right)\eta\right)\end{aligned} \tag{57}$$

$$\lambda_b^{*}=\left(M^2+i\Omega\right)a_{79} \tag{58}$$

$$\begin{aligned}f_{1a}^{*}\,Re=&\frac{2\lambda_a^{*}}{M^2}\left[a_{23}m_6\,exp\left(\frac{m_6}{4}\right)-a_{15}m_5\,exp\left(\frac{m_5}{4}\right)\right]+\\&\frac{2Gr}{Re}\left[a_{10}m_1\,exp\left(\frac{m_1}{4}\right)+a_{11}m_2\,exp\left(\frac{m_2}{4}\right)-a_{21}m_5\,exp\left(\frac{m_5}{4}\right)+a_{29}m_6\,exp\left(\frac{m_6}{4}\right)\right]+\\&4a_{12}m_1\,exp\left(\frac{m_1}{2}\right)+4a_{14}m_2\,exp\left(\frac{m_2}{2}\right)-2a_{22}m_5\,exp\left(\frac{m_5}{4}\right)+2a_{30}m_6\,exp\left(\frac{m_6}{4}\right)+\\&2a_{13}\left(m_1+m_2\right)exp\left(\frac{m_1+m_2}{4}\right)\end{aligned} \tag{59}$$

$$f_{2a}^{*}\,Re = -\frac{2\lambda_a^{*}}{M^2}\left[a_{23}m_6\,exp\left(-\frac{m_6}{4}\right)-a_{15}m_5\,exp\left(-\frac{m_5}{4}\right)\right]-$$
$$\frac{2Gr}{Re}\left[a_{10}m_1\,exp\left(-\frac{m_1}{4}\right)+a_{11}m_2\,exp\left(-\frac{m_2}{4}\right)-a_{21}m_5\,exp\left(-\frac{m_5}{4}\right)+a_{29}m_6\,exp\left(-\frac{m_6}{4}\right)\right]-$$
$$4a_{12}m_1\,exp\left(-\frac{m_1}{2}\right)-4a_{14}m_2\,exp\left(-\frac{m_2}{2}\right)+2a_{22}m_5\,exp\left(-\frac{m_5}{4}\right)-2a_{30}m_6\,exp\left(-\frac{m_6}{4}\right)-$$
$$2a_{13}\left(m_1+m_2\right)exp\left(-\frac{m_1+m_2}{4}\right) \tag{60}$$

$$f_{1b}^{*}\,Re = \frac{2\lambda_b^{*}}{M^2+i\Omega}\left[a_{62}m_8\,exp\left(\frac{m_8}{4}\right)-a_{52}m_7\,exp\left(\frac{m_7}{4}\right)\right]-2a_{47}m_3\,exp\left(\frac{m_3}{4}\right)+$$
$$2a_{46}m_4\,exp\left(\frac{m_4}{4}\right)-2a_{59}m_7\,exp\left(\frac{m_7}{4}\right)-2a_{67}m_8\,exp\left(\frac{m_8}{4}\right)+$$
$$2a_{48}\left(m_1+m_2\right)exp\left(\frac{m_1+m_2}{4}\right)-2a_{49}\left(m_1+m_3\right)exp\left(\frac{m_1+m_3}{4}\right)-$$
$$2a_{51}\left(m_2+m_3\right)exp\left(\frac{m_2+m_3}{4}\right)+2a_{50}\left(m_2+m_4\right)exp\left(\frac{m_2+m_4}{4}\right) \tag{61}$$

$$f_{2b}^{*}\,Re = -\frac{2\lambda_b^{*}}{M^2+i\Omega}\left[a_{62}m_8\,exp\left(-\frac{m_8}{4}\right)-a_{52}m_7\,exp\left(-\frac{m_7}{4}\right)\right]+2a_{47}m_3\,exp\left(-\frac{m_3}{4}\right)-$$
$$2a_{46}m_4\,exp\left(-\frac{m_4}{4}\right)+2a_{59}m_7\,exp\left(-\frac{m_7}{4}\right)+2a_{67}m_8\,exp\left(-\frac{m_8}{4}\right)-$$
$$2a_{48}\left(m_1+m_2\right)exp\left(-\frac{m_1+m_2}{4}\right)+2a_{49}\left(m_1+m_3\right)exp\left(-\frac{m_1+m_3}{4}\right)+$$
$$2a_{51}\left(m_2+m_3\right)exp\left(-\frac{m_2+m_3}{4}\right)-2a_{50}\left(m_2+m_4\right)exp\left(-\frac{m_2+m_4}{4}\right) \tag{62}$$

$$Nu_{1a}^{*} = -\left[a_6m_1\,exp\left(\frac{m_1}{4}\right)+a_7m_2\,exp\left(\frac{m_2}{4}\right)\right] \tag{63}$$

$$Nu_{2a}^{*} = -\left[a_6m_1\,exp\left(-\frac{m_1}{4}\right)+a_7m_2\,exp\left(-\frac{m_2}{4}\right)\right] \tag{64}$$

$$Nu_{1b}^{*} = a_9m_3\,exp\left(\frac{m_3}{4}\right)-a_8m_4\,exp\left(\frac{m_4}{4}\right) \tag{65}$$

$$Nu_{2b}^{*} = a_9m_3\,exp\left(-\frac{m_3}{4}\right)-a_8m_4\,exp\left(-\frac{m_4}{4}\right) \tag{66}$$

$$f_1\,Re = \text{Real part of}\left[f_{1a}^{*}\,Re+\frac{Gr}{Re}\,f_{1b}^{*}\,Re\,exp\left(i\tau\right)\right] \tag{67}$$

$$f_2\,Re = \text{Real part of}\left[f_{2a}^{*}\,Re+\frac{Gr}{Re}\,f_{2b}^{*}\,Re\,exp\left(i\tau\right)\right] \tag{68}$$

$$Nu_1 = \text{Real part of}\left[Nu_{1a}^{*}+Nu_{1b}^{*}\,exp\left(i\tau\right)\right] \tag{69}$$

$$Nu_2 = \text{Real part of}\left[Nu_{2a}^{*}+Nu_{2b}^{*}\,exp\left(i\tau\right)\right] \tag{70}$$

The critical values of Gr/Re can be acquired by equating the expressions of funning friction factors to zero at the channel walls because separation at the walls takes place when there is no drag force. The coefficients m_i, a_i are given in Appendix.

$$\left.\frac{Gr}{Re}\right|_{\eta=-1/4} = -\frac{f_{1a}^{*}\,Re}{f_{1b}^{*}\,Re\,exp\left(i\,\tau\right)} \tag{71}$$

$$\left.\frac{Gr}{Re}\right|_{\eta=1/4} = -\frac{f_{2a}^{*}\,Re}{f_{2b}^{*}\,Re\,exp(i\tau)} \tag{72}$$

4. Results and Discussion

The contributes of magnetic parameter M, suction parameter S, nonlinear Boussinesq approximation parameter C, mixed convection parameter Gr/Re, angular frequency Ω, Prandtl number Pr, heat generation parameter H, and time τ on the liquid motion U, temperature θ, fanning friction factor at the left wall $f_1 Re$, fanning friction factor at the right wall $f_2 Re$, heat transfer coefficient at the left wall Nu_1, heat transfer coefficient at the right wall Nu_2, and pressure drop λ are displayed in Figs.2 to 14 as well as tables 2 to 7. The present investigation has been implemented with the selected values of $\chi=1$, $S=1$, $Gr/Re=500$, $H=1$, $M=10$, $\tau=1$, $C=1$, $\Omega=50$, and $Pr=0.71$. In this study $C\neq 0$ denotes the nonlinear Boussinesq approximation and $Gr/Re>1$ implies natural convection dominates forced convection because Grashof number Gr is buoyancy parameter and Reynolds number Re is pressure driven parameter. The activity of non linear Boussinesq approximation parameter C is to escalate the achievement of reverse stream generation at the channel plates. We compared our results of λ with those of Jha and Oni (2020) as a special case by setting $C=1$, $\chi=1$, $Gr/Re=100$, $\Omega=10$, $Pr=0.71$, $\tau=0.1$, $S=0$, $M=0$, and $H=0$. It is revealed from Table 1 that, there is an excellent agreement between both the results.

Table 1: Comparison of critical values Gr/Re at the channel walls with Jha and Oni (2020).

Ω	Jha and Oni (2020)		Present	
	$\left.\frac{Gr}{Re}\right\|_{\eta=-1/4}$	$\left.\frac{Gr}{Re}\right\|_{\eta=1/4}$	$\left.\frac{Gr}{Re}\right\|_{\eta=-1/4}$	$\left.\frac{Gr}{Re}\right\|_{\eta=1/4}$
1	116.70	- 96.97	116.7000	- 96.9702
2	116.83	- 97.04	116.8301	- 97.0411
5	117.25	- 97.32	117.2520	- 97.3210
10	118.00	- 97.99	118.0001	- 97.9902
20	119.73	- 100.04	119.7311	- 100.0401
50	126.89	-109.84	126.8901	- 109.8410
100	150.11	- 129.83	150.1110	- 129.8311
200	365.30	- 170.86	365.1200	- 170.8602

Plots of liquid motion U corresponding to nonlinear Bousssinesq approximation parameter C are displayed in Fig. 2. The figure shows that the liquid motion escalates at the channel walls and declines in the central region of the channel with an enhancement of nonlinear Bousssinesq approximation parameter C. Fig. 3 depicts the impact of mixed convection parameter Gr/Re on the liquid motion U. In this study, it is identified that increasing the values of mixed convection parameter accelerate the liquid motion. It has been found that, the liquid motion is an increasing function of the mixed convection parameter. Fig.4. illustrates how angular frequency Ω affects the liquid motion U. The liquid motion behaves as a decreasing function of angular frequency at the channel walls and an increasing function of angular frequency in the central region of the channel. Fig. 5 shows the relationship between the Prandtl number Pr and the liquid motion U. This graph shows a decline in the liquid motion at the channel walls and an increase in the liquid motion in the central region of the channel with an enhancement in the Prandtl number. Fig. 6 displays a positive correlation between the suction parameter S and the liquid motion U. Hence the liquid motion enhanced when the suction parameter rises. Fig. 7 displays a negative correlation between the magnetic parameter M and the liquid motion U. Hence the liquid motion declined when the magnetic parameter rises. The clarification of this on the hydrodynamics is due to an increase in mechanical resistive force with an enhancement in magnetic parameter. Based on the data shown in Fig. 8, it can be observed that there is a negative correlation between the liquid motion U and the heat generation parameter H at the channel walls whereas there is a positive correlation between the liquid motion U and the heat generation parameter H in the central region of the channel. As the value of the heat generation parameter rises, the liquid motion depletes at the channel walls and escalates in the central region of the channel. Fig. 9 displays the mutation of the liquid motion U with the progress of time τ. It

is identified from this sketch that, the liquid motion U escalates with the progress of time τ at the channel walls while the liquid motion U depletes in the central region of the channel.

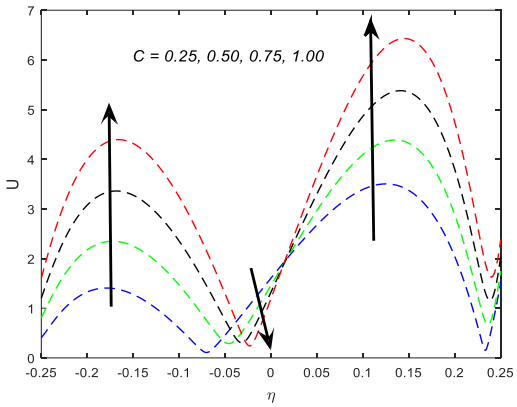

Fig. 2: Interpretation of liquid motion with respect to nonlinear Bousssinesq approximation

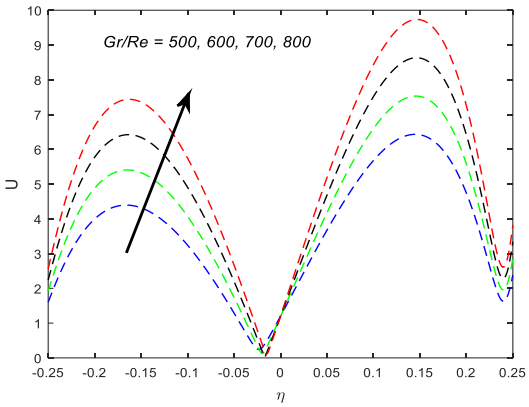

Fig. 3: Interpretation of liquid motion with respect to mixed convection parameter

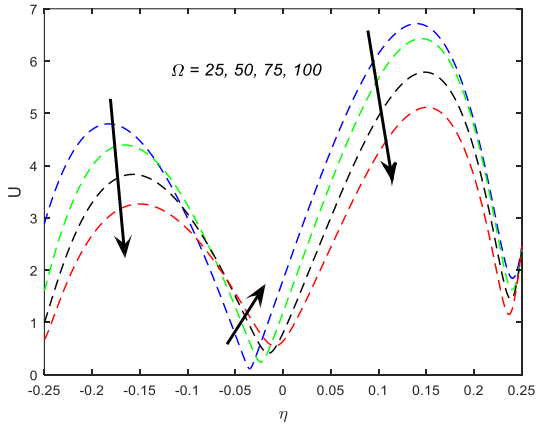

Fig. 4: Interpretation of liquid motion with respect to angular frequency

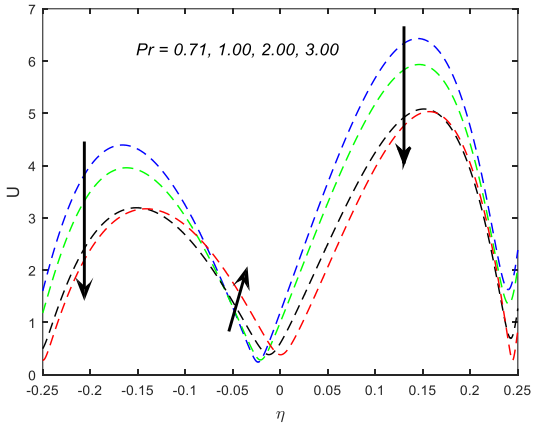

Fig. 5: Interpretation of liquid motion with respect to Prandtl number

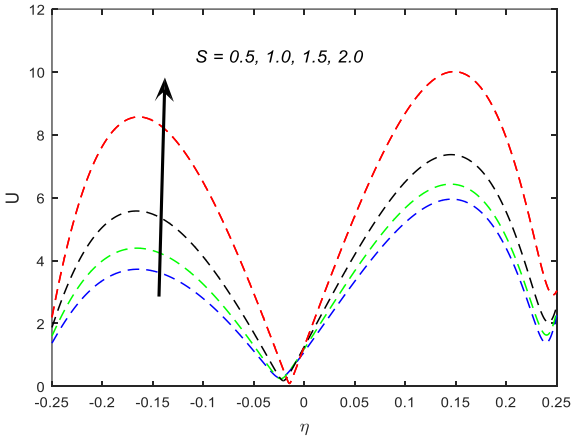

Fig. 6: Interpretation of liquid motion with respect to suction parameter

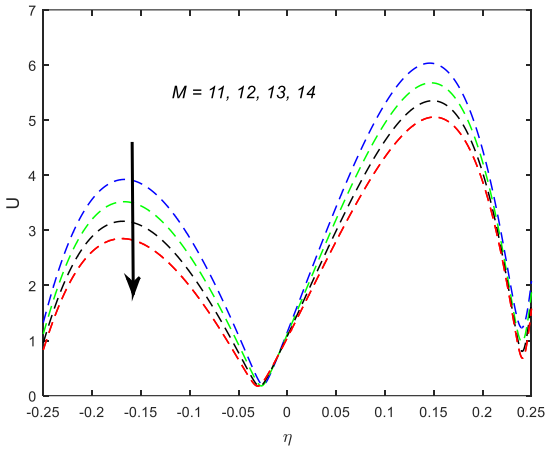

Fig. 7: Interpretation of liquid motion with respect to magnetic parameter

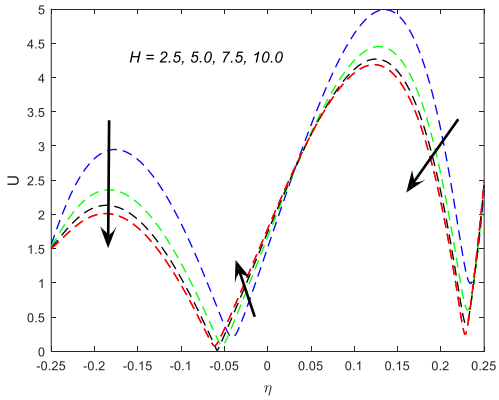

Fig. 8: Interpretation of liquid motion with respect to heat generation parameter

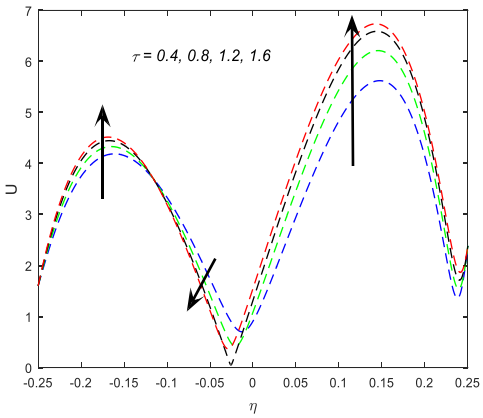

Fig. 9: Interpretation of liquid motion with respect to time

The mutation of the liquid temperature θ for distinct values of angular frequency Ω, Prandtl number Pr, and time τ is enumerated across the Figs. 10, 11, and 12 respectively. The analysis of these graphs indicate that, the liquid temperature θ accelerates at the channel left wall and depletes at the channel right wall with an enhancement in the parameters Ω, Pr, and τ. Fig. 13 displays the liquid temperature θ for various values of heat generation parameter H. It is noticed from this graph, the liquid temperature escalates as the heat generation parameter H increases. In Fig. 14, the liquid temperature θ escalates at the channel walls and depletes in the central region of the channel when the value of the suction parameter S rises.

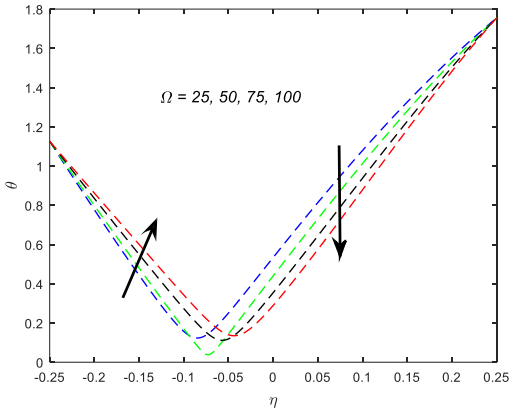

Fig. 10: Interpretation of liquid temperature with respect to angular frequency

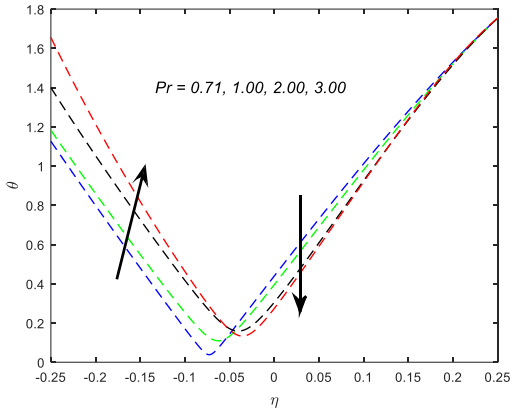

Fig. 11: Interpretation of liquid temperature with respect to Prandtl number

From Tables 2 and 3, it is memorialized that, the fanning friction factor at the left wall $f_1 Re$ depletes by escalating the mixed convection parameter Gr / Re, suction parameter S, nonlinear Boussinesq approximation parameter C, and time τ whereas it accelerates by raising the magnetic parameter M, Prandtl number Pr, and heat generation parameter H. The fanning friction factor at the left wall $f_1 Re$ depletes when $\Omega \in [25,50]$ and escalates when $\Omega \in [75,100]$. The fanning friction factor at the right wall $f_2 Re$ accelerates by escalating the magnetic parameter M, Prandtl number Pr, heat generation parameter H, and time τ whereas it depletes by rising the mixed convection parameter Gr / Re, angular frequency Ω, suction parameter S, and nonlinear Boussinesq approximation parameter C.

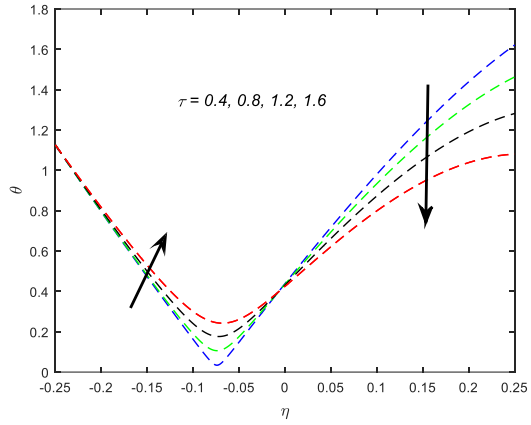

Fig. 12: Interpretation of liquid temperature with respect to time

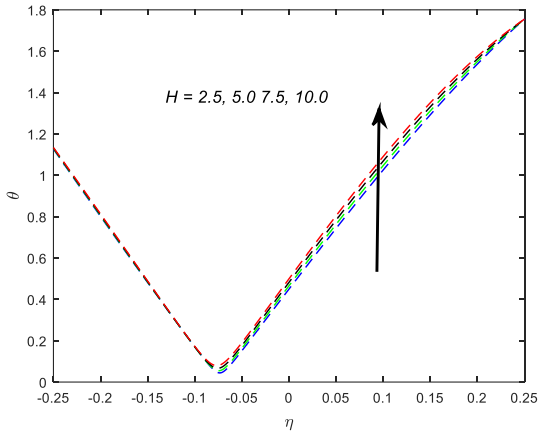

Fig. 13: Interpretation of liquid temperature with respect to heat generation parameter

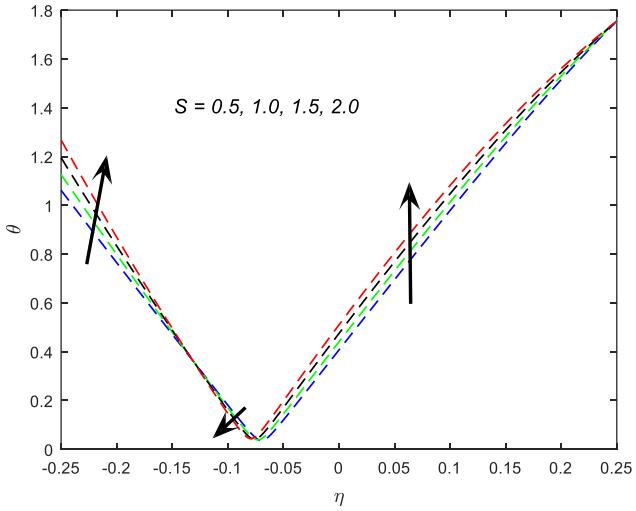

Fig. 14: Interpretation of liquid temperature with respect to suction parameter

Table 2: Fanning friction factor at the channel left and right plates with respect to Gr/Re , Ω , M , and S .

Gr / Re	Ω	M	S	$f_1 Re$	$f_2 Re$
500	50	10	1.0	-119.7970	-650.1188
600	50	10	1.0	-150.6083	-786.3747
700	50	10	1.0	-181.4196	-922.6306
800	50	10	1.0	-212.2309	-1058.9030
500	25	10	1.0	-109.0675	-484.1303
500	50	10	1.0	-119.7970	-650.1188
500	75	10	1.0	-93.6021	-773.4724
500	100	10	1.0	-65.0072	-871.4848
500	50	11	1.0	-115.2815	-565.4910
500	50	12	1.0	-109.4941	-498.4063
500	50	13	1.0	-103.0585	-443.8459
500	50	14	1.0	-96.3434	-398.5318
500	50	10	0.5	-103.0115	-640.0819
500	50	10	1.0	-119.7970	-650.1188
500	50	10	1.5	-149.4925	-721.5311
500	50	10	2.0	-226.1164	-994.8265

Table 3: Fanning friction factor at the channel left and right plates with respect to C , H , Pr , and τ .

C	Pr	H	τ	$f_1 Re$	$f_2 Re$
0.25	0.71	1.0	1.0	-68.1828	-120.6418
0.50	0.71	1.0	1.0	-85.3876	-297.1341
0.75	0.71	1.0	1.0	-102.5923	-473.6265
1.00	0.71	1.0	1.0	-119.7970	-650.1188
1.00	0.71	1.0	1.0	-119.7970	-650.1188
1.00	1.00	1.0	1.0	-103.7219	-545.5067
1.00	2.00	1.0	1.0	-67.2340	-265.9615
1.00	3.00	1.0	1.0	-40.8411	-191.4627
1.00	0.71	2.5	1.0	-84.3879	-344.4778
1.00	0.71	5.0	1.0	-70.5611	-193.4531
1.00	0.71	7.5	1.0	-66.4995	-122.7293
1.00	0.71	10.0	1.0	-65.5459	-78.3385
1.00	0.71	1.0	0.4	-53.4688	-720.5566
1.00	0.71	1.0	0.8	-99.9298	-705.6885
1.00	0.71	1.0	1.2	-136.3321	-564.9903
1.00	0.71	1.0	1.6	-156.9285	-320.6754

From Tables 4 and 5, it is remarked that, the pressure drop λ accelerates by raising the mixed convection parameter Gr / Re , angular frequency Ω , suction parameter S , nonlinear Boussinesq approximation parameter C , and time τ whereas it depletes by escalating the magnetic parameter M , Prandtl number Pr , and heat generation parameter H .

Table 4: Pressure drop with respect to Gr/Re , Ω , M , and S .

Gr / Re	Ω	M	S	λ
500	50	10	1.0	252.2238
600	50	10	1.0	297.7657
700	50	10	1.0	345.8844
800	50	10	1.0	395.6408
500	25	10	1.0	250.8791
500	50	10	1.0	252.2238
500	75	10	1.0	275.2855
500	100	10	1.0	300.5498
500	50	11	1.0	228.4669
500	50	12	1.0	213.2151
500	50	13	1.0	202.9702
500	50	14	1.0	195.9729
500	50	10	0.5	230.4328
500	50	10	1.0	252.2238
500	50	10	1.5	287.1591
500	50	10	2.0	371.6406

Table 5: Pressure drop with respect to C , Pr , H , and τ .

C	Pr	H	τ	λ
0.25	0.71	1.0	1.0	105.8189
0.50	0.71	1.0	1.0	154.6171
0.75	0.71	1.0	1.0	203.4196
1.00	0.71	1.0	1.0	252.2238
1.00	0.71	1.0	1.0	252.2238
1.00	1.00	1.0	1.0	208.3932
1.00	2.00	1.0	1.0	111.2056

1.00	3.00	1.0	1.0	56.3706
1.00	0.71	2.5	1.0	216.4152
1.00	0.71	5.0	1.0	201.1501
1.00	0.71	7.5	1.0	195.0811
1.00	0.71	10.0	1.0	192.0678
1.00	0.71	1.0	0.4	161.4453
1.00	0.71	1.0	0.8	221.5180
1.00	0.71	1.0	1.2	281.8583
1.00	0.71	1.0	1.6	335.2474

From Tables 6 and 7 it is identified that, the heat transfer coefficient at the left wall Nu_1 decelerates by raising the angular frequency Ω and heat generation parameter H whereas it accelerates by escalating the suction parameter S and Prandtl number Pr. Rate of heat transfer Nu_1 enhances when $\tau \in [0.4,1.2]$ and depletes when $\tau \in [1.2,1.6]$. The heat transfer coefficient at the right wall Nu_2 depletes by raising the angular frequency Ω, suction parameter S, Prandtl number Pr, heat generation parameter H, and time τ.

Table 6: Heat transfer coefficient at the channel left and right plates with respect to Ω, S, and Pr.

Ω	S	Pr	Nu_1	Nu_2
25	1.0	0.71	7.1103	2.4646
50	1.0	0.71	6.6517	1.8325
75	1.0	0.71	5.9270	1.6109
100	1.0	0.71	5.3645	1.4373
50	0.5	0.71	5.9631	2.1462
50	1.0	0.71	6.6517	1.8325
50	1.5	0.71	7.4074	1.5323
50	2.0	0.71	8.2351	1.2457
50	1.0	0.71	6.6517	1.8325
50	1.0	1.00	6.6021	1.3478
50	1.0	2.00	7.2141	-0.1072
50	1.0	3.00	9.3803	-1.4575

Table 7: Heat transfer coefficient at the channel left and right plates with respect to H and τ.

H	τ	Nu_1	Nu_2
2.5	1.0	6.6048	1.6373
5.0	1.0	6.5258	1.3072
7.5	1.0	6.4455	0.9715
10.0	1.0	6.3630	0.6306
1.0	0.4	6.0537	5.1668
1.0	0.8	6.5103	2.9372
1.0	1.2	6.7268	0.7934
1.0	1.6	6.6689	-0.9264

5. Conclusions

This article presents the time periodic nonlinear unsteady flow in an inclined channel in the proximity of suction and heat generation. The main observations can be abstracted as:

- The incorporation of nonlinear Bousssinesq simulation delivers a more logical implication to the real life situation refers to while a linear Bousssinesq simulation is used.
- Escalate in angular frequency, Prandtl number, and heat generation parameter declines the motion of the liquid at the channel left and right plates whereas escalates the motion of the liquid in the central region of the channel.

- Escalate in nonlinear Boussinesq approximation parameter and time accelerates the motion of the liquid at the channel left and right plates whereas depletes the motion of the liquid in the central region of the channel.
- The fanning friction factor rises at the channel left and right plates with increasing values of magnetic parameter, Prandtl number, and heat generation parameter whereas it declines at the channel left and right plates with an enhancement in mixed convection parameter, suction parameter, and nonlinear Boussinesq approximation parameter.
- Progress of time declines the fanning friction at the channel left plate whereas the revere direction is identified at the channel right plate.
- The pressure drop exhibit a positive correlation with the mixed convection parameter, angular frequency, suction parameter, nonlinear Boussinesq approximation parameter, and time. As the magnetic parameter, Prandtl number, and heat generation parameter increases, the pressure drop shows down.

These findings will facilitate further research on slip or no-slip conditions, stress jump conditions, chemical interactions, and proximity to porous media, Nanofluids, Micropolar fluids. Such research holds significant applications in the mechanical engineering industry.

References

Adem, G. A., and Chanie, A. G. (2024): Influence of suction and injection on the electrical magnetohydrodynamic behavior of nanofluid in a nonlinear radiative flow over an extending surface. Numerical Heat Transfer, Part B: Fundamentals, vol. 85, pp. 1-24. https://doi.org/10.1080/10407790.2024.2348766

Avci, M., and Aydin, O. (2007): Mixed convection in a vertical parallel plate microchannel with asymmetric wall heat fluxes. ASME Journal of Heat Transfer, vol. 129, pp. 1091-1095. https://doi.org/10.1115/1.2737483

Barletta, A., and Zanchini, E. (2003): Time-periodic laminar mixed convection in an inclined channel, International Journal of Heat and Mass Transfer, vol. 46, no. 3, pp. 551-563. https://doi.org/10.1016/S0017-9310(02)00290-9

Fardi, M., Pishkar, I., Alidousti, J., and Khan, Y. (2021): Numerical investigation of the MHD suction–injection model of viscous fluid using a kernel-based method, Archive of Applied Mechanics, vol. 91, no. 10, pp. 4205-4221. https://doi.org/10.1007/s00419-021-02003-2

Hamza, M. M., Ojemeri, G., and Abdulsalam, S. (2019): Mixed convection flow of viscous reactive fluids with thermal diffusion and radial magnetic field in a vertical porous annulus, Computational Mathematics Modeling, vol. 30, pp. 239-253. https://doi.org/10.1007/s10598-019-09451-0

Indira, S, and Raju R. S (2023): Analytical study of MHD mixed convection flow for Maxwell Nanofluid through a vertical cone with porous material in the presence of variable thermal conductivity and Soret, Dufour effects, Journal of Advanced Research in Fluid Mechanics and Thermal Sciences, vol. 106, no. 2, pp. 129-142. https://doi.org/10.37934/arfmts.106.2.129142

Jha, B. K., and Oni, M. O. (2020): Nonlinear mixed convection flow in an inclined channel with time periodic boundary conditions, International Journal of Applied and Computational Mathematics, vol. 6, Article No: 129, pp. 1-17. https://doi.org/10.1007/s40819-020-00880-9

Jha, B. K., Daramola, D., and Ajibade, A. G. (2015): Mixed convection in an inclined channel filled with porous material having time-periodic boundary conditions: steady-periodic regime, Transport in Porous Media, vol. 109, no. 2, pp. 495-512. DOI: 10.1007/s11242-015-0533-6

Jha, B. K., Jibril, H. M., and Yusuf, K. L.(2022): Run up flow of MHD fluid between parallel porous plates in the presence of transverse magnetic field, Heat Transfer, vol. 52, no. 3, 2561-2670. https://doi.org/10.1002/htj.22799

Kumar, V. S. S., Devaki, B., and Pai, N. P. (2024): Analysis of MHD and heat transfer characteristics of thermally radiative upper convected Maxwell fluid flow between moving plates: semi-analytical and numerical solution, CFD Letters, vol. 16, no. 4, pp. 39-53. https://doi.org/10.37934/cfdl.16.4.3953

Makinde, O. D., and Onyejekwe, O. O. (2011): A numerical study of MHD generalized Couette flow and heat transfer with variable viscosity and electrical conductivity, Journal of magnetism and magnetic materials, vol. 323, pp. 2757-2763. https://doi.org/10.1016/j.jmmm.2011.05.040

Makinde, O. D., Venkateswarlu, M., and Monaledi, R. L. (2018): Unsteady MHD flow of radiating and rotating fluid with Hall current and thermal diffusion past a moving plate in a porous medium, Defect and Diffusion Forum, vol. 389, pp. 71-85. https://doi.org/10.4028/www.scientific.net/DDF.389.71

Marzieh, K., Lyazid, D., and Sedat, T. (2021): Combined effect of roughness and suction on heat transfer in a laminar channel flow, International Communications in Heat and Mass Transfer, vol. 126, Article ID: 105377. https://doi.org/10.1016/j.icheatmasstransfer.2021.105377

Meduri, P. K., and Devi, P. N. L. (2024): Stokes flow past a contaminated fluid sphere embedded in a porous medium with slip condition. Arch. Mech, vol. 76, no. 3, pp. 253-275. DOI: 10.24423/aom.4392

Nagesh, G., and Raghunath, K. (2022): Soret radiation and chemical reaction effect on MHD Jeffrey fluid flow past an inclined vertical plate embedded in porous medium, Materials Today: Proceedings, vol. 50, pp. 2218-2226.https://doi.org/10.1016/j.matpr.2021.09.480

Narasimhan, M. N. L. (2011): On the flow of an electrically conducting nonlocal viscous fluid between parallel plates in the presence of a transverse magnetic field in magnetohydrodynamics, International journal of engineering science, vol. 49, pp.1470-1476. https://doi.org/10.1016/j.ijengsci.2011.02.009

Obalalu, A. M., Wahaab, F. A., and Adebayo, L. L. (2020): Heat transfer in an unsteady vertical porous channel with injection/suction in the presence of heat generation, Journal of Taibah University for Science, vol. 14, no. 1, pp. 541-548. https://doi.org/10.1080/16583655.2020.1748844

Prasad, T. R. K. D. V., Linga Raju, T., and Rajakumar, K. V. B. (2023): Viscous dissipation and radiation absorption effects on unsteady MHD free convective fluid flow past an inclined porous plate with chemical reaction. Heat Transfer, vol. 52, pp. 1254-1274. doi:10.1002/htj.22739

Raghunath, K., Obulesu, M., and Raju, K. V. (2023): Radiation absorption on MHD free conduction flow through porous medium over an unbounded vertical plate with heat source, International Journal of Ambient Energy, vol. 44, no.1, pp. 1712-1720. https://doi.org/10.1080/01430750.2023.2181869

Raghunatha, K. R., and Vinod, Y. (2023): Effects of heat transfer on MHD suction–injection model of viscous fluid flow through differential transformation and Bernoulli wavelet techniques, Heat Transfer, vol. 52, no.7, pp. 4914-4945. https://doi.org/10.1002/htj.22911

Rajakumar, K. V. B., Sreenivasulu, G., and Balamurugan, K. S. (2024): Influence of heat flow due to concentration gradient on unsteady MHD heat and mass transform dissipative flow with spanwise fluctuating temperature. Numerical Heat Transfer, Part A: Applications, pp. 1-26. https://doi.org/10.1080/10407782.2024.2364061

Reddy, P. S., and Sreedevi, P. (2024) Enhanced entropy generation and heat transfer characteristics of magnetic nano-encapsulated phase change materials in latent heat thermal energy storage systems. Appl. Math. Mech.-Engl. Ed, vol. 45, pp. 1051-1070. https://doi.org/10.1007/s10483-024-3126-9

Sivaprasad, J., and Kumar, M. P., (2025); Exact solution for laminar viscous fluid flow over a contaminated liquid drop placed in a porous region: Magnetohydrodynamics. Physics of Fluids, vol. 37, no. 1, Article ID: 013626. https://doi.org/10.1063/5.0251114

Susmita, D., Santanu, R., and Kumar, M. K. (2024): Analyzing the effects of suction and injection Reynolds number on the transport process in a hydromagnetic flow through a channel of reactive porous walls, Chinese Journal of Physics, vol. 87, pp. 510-524. https://doi.org/10.1016/j.cjph.2023.12.022

Venkateswarlu, M., and Lakshmi, D. V. (2017): Thermal diffusion, hall current and chemical reaction effects on unsteady MHD natural convective flow past a vertical plate, U. P. B. Sci. Bull., Series D: Mechanical Engineering, vol. 79, no. 1, pp. 91-106.
https://www.scientificbulletin.upb.ro/rev_docs_arhiva/fulla72_990725.pdf

Venkateswarlu, M., and Lakshmi, D. V. (2021): Diffusion-thermo and heat source effects on the unsteady radiative MHD boundary layer slip flow past an infinite vertical porous plate, Journal of Naval Architecture and Marine Engineering, vol. 18, no. 1, pp. 55-72. https://doi.org/10.3329/jname.v18i1.33024

Venkateswarlu, M., and Makinde, O. D (2018): Unsteady MHD slip flow with radiative heat and mass transfer over an inclined plate embedded in a porous medium, Defect and Diffusion Forum, vol. 384, pp. 31-48. https://doi.org/10.4028/www.scientific.net/DDF.384.31

Venkateswarlu, M., and Kumar, M. P. (2017): Soret and heat source effects on MHD flow of a viscous fluid in a parallel porous plate channel in presence of slip condition, U. P. B. Sci. Bull., Series D: Mechanical Engineering, vol. 79, no. 4, pp. 171-186.
https://www.scientificbulletin.upb.ro/rev_docs_arhiva/fullf50_220170.pdf

Venkateswarlu, M., Lakshmi, D. V., and Makinde, O. D. (2020): Thermodynamics analysis of Hall current and Soret number on hydromagnetic couette flow in a rotating system with a convective boundary condition, Heat Transfer Research, vol. 51, no. 1, pp. 83-101. http://dx.doi.org/10.1615/HeatTransRes.2019027139

Venkateswarlu, M., Kumar, M. P., and Makinde, O. D., (2022): Establishment of impulsive and accelerated motions of Casson fluid in an inclined plate in the proximity of MHD and heat generation, Periodica Polytechnica Mechanical Engineering, vol. 66, no. 3, pp. 219-230. https://doi.org/10.3311/PPme.19424

Venkateswarlu, M., Reddy, P. R., and Lakshmi, K. J. (2024): Analytical study of Soret and Dufour effects on heat destructive Casson liquid movement past an infinite vertical plate, Journal of Naval Architecture and Marine Engineering, vol. 21, no. 4, pp. 27-40. http://dx.doi.org/10.3329/jname.v21i1.69228

Appendix

$$m_1=\frac{S\,Pr+\sqrt{S^2\,Pr^2-4H\,Pr}}{2},\ m_2=\frac{S\,Pr-\sqrt{S^2\,Pr^2-4H\,Pr}}{2},\ m_3=\frac{S\,Pr+\sqrt{S^2\,Pr^2-4\left(H-i\Omega\right)Pr}}{2},$$

$$m_4=\frac{S\,Pr-\sqrt{S^2\,Pr^2-4\left(H-i\Omega\right)Pr}}{2},\ m_5=\frac{S+\sqrt{S^2+4M^2}}{2},\ m_6=\frac{S-\sqrt{S^2+4M^2}}{2},$$

$$m_7=\frac{S+\sqrt{S^2+4\left(M^2+i\Omega\right)}}{2},\ m_8=\frac{S-\sqrt{S^2+4\left(M^2+i\Omega\right)}}{2},\ a_1=\frac{1}{m_1}exp\left(\frac{m_2}{4}\right)sinh\left(\frac{m_1}{4}\right),$$

$$a_2=\frac{1}{m_2}exp\left(\frac{m_1}{4}\right)sinh\left(\frac{m_2}{4}\right),\ a_3=\frac{1}{m_1}exp\left(-\frac{m_2}{4}\right)sinh\left(\frac{m_1}{4}\right),\ a_4=\frac{1}{m_2}exp\left(-\frac{m_1}{4}\right)sinh\left(\frac{m_2}{4}\right),\ a_5=\frac{a_1-a_2}{a_3-a_4},$$

$$a_6=\frac{a_5\,exp\left(-\frac{m_2}{4}\right)-exp\left(\frac{m_2}{4}\right)}{2\,sinh\left(\frac{m_1-m_2}{4}\right)},\ a_7=\frac{exp\left(\frac{m_1}{4}\right)-a_5\,exp\left(-\frac{m_1}{4}\right)}{2\,sinh\left(\frac{m_1-m_2}{4}\right)},\ a_8=\frac{exp\left(\frac{m_3}{4}\right)}{2\,sinh\left(\frac{m_3-m_4}{4}\right)},\ a_9=\frac{exp\left(\frac{m_4}{4}\right)}{2\,sinh\left(\frac{m_3-m_4}{4}\right)},$$

$$a_{10}=\frac{a_6}{m_1^2-s\,m_1-M^2},\ a_{11}=\frac{a_7}{m_2^2-s\,m_2-M^2},\ a_{12}=\frac{C\,a_6^2}{4m_1^2-2s\,m_1-M^2},\ a_{13}=\frac{2C\,a_6\,a_7}{\left(m_1+m_2\right)^2-s\left(m_1+m_2\right)-M^2},$$

$$a_{14}=\frac{C\,a_7^2}{4m_2^2-2s\,m_2-M^2},\ a_{15}=\frac{sinh\left(\frac{m_6}{4}\right)}{sinh\left(\frac{m_5-m_6}{4}\right)},\ a_{16}=\frac{a_{10}\,sinh\left(\frac{m_1-m_6}{4}\right)}{sinh\left(\frac{m_5-m_6}{4}\right)},\ a_{17}=\frac{a_{11}\,sinh\left(\frac{m_2-m_6}{4}\right)}{sinh\left(\frac{m_5-m_6}{4}\right)},$$

$$a_{18}=\frac{a_{12}\,sinh\left(\frac{2m_1-m_6}{4}\right)}{sinh\left(\frac{m_5-m_6}{4}\right)},\ a_{19}=\frac{a_{13}\,sinh\left(\frac{m_1+m_2-m_6}{4}\right)}{sinh\left(\frac{m_5-m_6}{4}\right)},\ a_{20}=\frac{a_{14}\,sinh\left(\frac{2m_2-m_6}{4}\right)}{sinh\left(\frac{m_5-m_6}{4}\right)},\ a_{21}=a_{16}+a_{17},$$

$$a_{22}=a_{18}+a_{19}+a_{20},\ a_{23}=\frac{sinh\left(\frac{m_5}{4}\right)}{sinh\left(\frac{m_5-m_6}{4}\right)},\ a_{24}=\frac{a_{10}\,sinh\left(\frac{m_1-m_5}{4}\right)}{sinh\left(\frac{m_5-m_6}{4}\right)},\ a_{25}=\frac{a_{11}\,sinh\left(\frac{m_2-m_5}{4}\right)}{sinh\left(\frac{m_5-m_6}{4}\right)},$$

$$a_{26}=\frac{a_{12}\,sinh\left(\frac{2m_1-m_5}{4}\right)}{sinh\left(\frac{m_5-m_6}{4}\right)},\ a_{27}=\frac{a_{13}\,sinh\left(\frac{m_1+m_2-m_5}{4}\right)}{sinh\left(\frac{m_5-m_6}{4}\right)},\ a_{28}=\frac{a_{14}\,sinh\left(\frac{2m_2-m_5}{4}\right)}{sinh\left(\frac{m_5-m_6}{4}\right)},\ a_{29}=a_{24}+a_{25},$$

$$a_{30}=a_{26}+a_{27}+a_{28},\ a_{31}=\frac{sinh\left(\frac{m_1}{2}\right)}{m_1},\ a_{32}=\frac{sinh\left(\frac{m_2}{2}\right)}{m_2},\ a_{33}=\frac{sinh\left(\frac{m_1}{4}\right)}{m_1},\ a_{34}=\frac{sinh\left(\frac{m_2}{4}\right)}{m_2},$$

$$a_{35}=\frac{sinh\left(\frac{m_1+m_2}{4}\right)}{m_1+m_2},\ a_{36}=\frac{sinh\left(\frac{m_5}{4}\right)}{m_5},\ a_{37}=\frac{sinh\left(\frac{m_6}{4}\right)}{m_6},\ a_{38}=\frac{1}{2}+2\left[a_{15}a_{36}-a_{23}a_{37}\right],$$

$$a_{39}=2\left[a_{21}a_{36}-a_{29}a_{37}-a_{10}a_{33}-a_{11}a_{34}\right],\ a_{40}=2\left[a_{22}a_{36}-a_{30}a_{37}-a_{13}a_{35}\right],\ a_{41}=a_{12}a_{31}+a_{14}a_{32},$$

$a_{42} = a_{40} - a_{41}$, $a_{43} = \frac{1}{2} - a_{42}$, $a_{44} = \frac{a_{43}}{a_{38}}$, $a_{45} = \frac{a_{39}}{a_{38}}$, $a_{46} = \frac{a_8}{m_4^2 - s\,m_4 - \left(M^2 + i\Omega\right)}$, $a_{47} = \frac{a_9}{m_3^2 - s\,m_3 - \left(M^2 + i\Omega\right)}$,

$a_{48} = \frac{2C\,a_6\,a_8}{\left(m_1 + m_4\right)^2 - s\left(m_1 + m_4\right) - \left(M^2 + i\Omega\right)}$, $a_{49} = \frac{2C\,a_6\,a_9}{\left(m_1 + m_3\right)^2 - s\left(m_1 + m_3\right) - \left(M^2 + i\Omega\right)}$,

$a_{50} = \frac{2C\,a_7\,a_8}{\left(m_2 + m_4\right)^2 - s\left(m_2 + m_4\right) - \left(M^2 + i\Omega\right)}$, $a_{51} = \frac{2C\,a_7\,a_9}{\left(m_2 + m_3\right)^2 - s\left(m_2 + m_3\right) - \left(M^2 + i\Omega\right)}$, $a_{52} = \frac{sinh\left(\frac{m_8}{4}\right)}{sinh\left(\frac{m_7 - m_8}{4}\right)}$,

$a_{53} = \frac{a_{46}\,sinh\left(\frac{m_4 - m_8}{4}\right)}{sinh\left(\frac{m_7 - m_8}{4}\right)}$, $a_{54} = \frac{a_{47}\,sinh\left(\frac{m_3 - m_8}{4}\right)}{sinh\left(\frac{m_7 - m_8}{4}\right)}$, $a_{55} = \frac{a_{48}\,sinh\left(\frac{m_1 + m_2 - m_8}{4}\right)}{sinh\left(\frac{m_7 - m_8}{4}\right)}$ $a_{56} = \frac{a_{49}\,sinh\left(\frac{m_1 + m_3 - m_8}{4}\right)}{sinh\left(\frac{m_7 - m_8}{4}\right)}$,

$a_{57} = \frac{a_{50}\,sinh\left(\frac{m_1 + m_4 - m_8}{4}\right)}{sinh\left(\frac{m_7 - m_8}{4}\right)}$, $a_{58} = \frac{a_{51}\,sinh\left(\frac{m_2 + m_3 - m_8}{4}\right)}{sinh\left(\frac{m_7 - m_8}{4}\right)}$, $a_{59} = \left(a_{53} + a_{55} + a_{57}\right) - \left(a_{54} + a_{56} + a_{58}\right)$,

$a_{60} = \frac{sinh\left(\frac{m_7}{4}\right)}{sinh\left(\frac{m_7 - m_8}{4}\right)}$, $a_{61} = \frac{a_{46}\,sinh\left(\frac{m_4 - m_7}{4}\right)}{sinh\left(\frac{m_7 - m_8}{4}\right)}$, $a_{62} = \frac{a_{47}\,sinh\left(\frac{m_3 - m_7}{4}\right)}{sinh\left(\frac{m_7 - m_8}{4}\right)}$, $a_{63} = \frac{a_{48}\,sinh\left(\frac{m_1 + m_2 - m_7}{4}\right)}{sinh\left(\frac{m_7 - m_8}{4}\right)}$,

$a_{64} = \frac{a_{49}\,sinh\left(\frac{m_1 + m_3 - m_7}{4}\right)}{sinh\left(\frac{m_7 - m_8}{4}\right)}$, $a_{65} = \frac{a_{50}\,sinh\left(\frac{m_2 + m_4 - m_7}{4}\right)}{sinh\left(\frac{m_7 - m_8}{4}\right)}$, $a_{66} = \frac{a_{51}\,sinh\left(\frac{m_2 + m_3 - m_7}{4}\right)}{sinh\left(\frac{m_7 - m_8}{4}\right)}$,

$a_{67} = \left(a_{62} + a_{64} + a_{66}\right) - \left(a_{61} + a_{63} + a_{65}\right)$, $a_{68} = \frac{sinh\left(\frac{m_3}{4}\right)}{m_3}$, $a_{69} = \frac{sinh\left(\frac{m_4}{4}\right)}{m_4}$, $a_{70} = \frac{sinh\left(\frac{m_7}{4}\right)}{m_7}$, $a_{71} = \frac{sinh\left(\frac{m_8}{4}\right)}{m_8}$,

$a_{72} = \frac{sinh\left(\frac{m_1 + m_2}{4}\right)}{m_1 + m_2}$, $a_{73} = \frac{sinh\left(\frac{m_1 + m_3}{4}\right)}{m_1 + m_3}$, $a_{74} = \frac{sinh\left(\frac{m_2 + m_3}{4}\right)}{m_2 + m_3}$, $a_{75} = \frac{sinh\left(\frac{m_2 + m_4}{4}\right)}{m_2 + m_4}$,

$a_{76} = \frac{1}{2} + 2\left[a_{52}a_{70} - a_{62}a_{71}\right]$, $a_{77} = 2\left[a_{47}a_{68} + a_{59}a_{70} + a_{67}a_{71} + a_{49}a_{73} + a_{51}a_{74}\right]$, $a_{78} = 2\left[a_{46}a_{69} + a_{48}a_{72} + a_{50}a_{75}\right]$

, $a_{79} = \frac{a_{78} - a_{77}}{a_{76}}$.